Measuring R_c with exclusive c-hadron decays and an outlook to A_{FB}^c, R_s, and A_{FB}^s at FCC-ee

Lars Röhrig,[a,b] **Jaiveer Singh Dutta,**[c] **Andreas Werner Jung,**[c] **Stéphane Monteil**[b]

[a] *Department of Physics, TU Dortmund University, Dortmund, Germany*
[b] *Université Clermont-Auvergne, CNRS, LPCA, 63000 Clermont-Ferrand, France*
[c] *Department of Physics & Astronomy, Purdue University, 525 Northwestern Ave, West Lafayette, IN, 47907, USA*

E-mail: lars.roehrig@tu-dortmund.de

Abstract: This analysis note is meant to be a telegraphic transcript of an ongoing analysis aimed at assessing the precision that can be reached at FCC-ee for the partial-width measurement of $Z \to c\bar{c}$. Intermediate results are also presented for the c-quark forward-backward asymmetry. Furthermore, it highlights the idea of measuring R_s and A_{FB}^s with exclusively reconstructed strange hadrons.

Contents

1 Introduction

The discovery of the Higgs boson at CERN's Large Hadron Collider (LHC) in 2012 completed the Standard Model (SM) of particle physics [1, 2]. Over the past decades, the SM has passed numerous precision tests in large collider experiments and remains the most comprehensive theory of fundamental interactions. However, despite its successes, the SM fails to account for phenomena such as dark matter and the matter-antimatter asymmetry in the universe.

These gaps motivate physicists to push the boundaries of precision measurements, aiming to study particle properties with even greater accuracy. In particular, the interaction between the Z boson and the heaviest fermions of the SM is expected to be highly sensitive to effects from physics beyond the SM (BSM). Yet, the most precise benchmarks in this area are still based on measurements from the Large Electron Positron (LEP) collider, which operated until 2000. LEP explored the electroweak (EW) interaction with centre-of-mass energies ranging from $\sqrt{s} \approx m_Z$ to $\sqrt{s} = 209\,\text{GeV}$. From around $2 \cdot 10^7$ Z boson decays, fundamental SM parameters such as the weak mixing angle $\sin^2(\theta_\text{W})$ were determined with a precision of 0.1 %. Moreover, the combined LEP and SLD data revealed a $2.9\,\sigma$ tension with the SM prediction of the beauty-quark forward-backward asymmetry A_{FB}^{b}. In response to these challenges, the scientific community is turning to the next-generation

lepton collider, expected to produce $\mathcal{O}(10^{12})$ Z-boson decays in a circular design with a circumference of 91 km. This design is proposed as part of the Future Circular Collider (FCC), specifically the electron-positron collider (FCC-ee), which will operate at energy stages ranging from $\sqrt{s} = m_Z$ to the $t\bar{t}$ threshold [3]. The vast number of Z boson decays would enable unprecedented precision in the study of electroweak precision observables (EWPO) among all types of fermions. However, a new method of identifying the flavour of beauty quarks has been proposed by the authors in Ref. [4], which is based on the exclusive reconstruction of beauty hadrons in the event to unambiguously tag the charge and flavour of the hemisphere. The application of the concept for precision measurements in the charm-quark sector to overcome systematic limitations in R_c and possibly A_{FB}^c is presented in the subsequent paper, which is structured as follows: Sec. 2 motivates the measurement of EWPOs at FCC-ee, before a new charm-tagger is introduced in Sec. 3. The performance and systematic uncertainties are discussed in Secs. 4 and 5, respectively. Sec. 6 presents the idea of applying the charm-tagger for the measurement of A_{FB}^c. The concept of measuring EWPOs in the strange sector is highlighted in Sec. 7 before the note concludes in Sec. 8.

2 Motivation for EWPO measurements at FCC-ee

The Z-pole operation at FCC-ee offers an immense portfolio for precision measurements across all fermions. Nevertheless, methods that go beyond the current state-of-the-art have to be developed in order to reduce not only the statistical precision but also the systematic uncertainty at a competitive level. The fruitful synergy of flavour-physics concepts and measurements of EW observables has been demonstrated in Ref. [4], bringing the total relative uncertainty of R_b and A_{FB}^b at the level of 0.015 % (factor 20 improvement) and 0.03 % (factor 50 improvement), respectively. This immense reduction of the uncertainty has motivated the use of exclusively reconstructed hadrons to measure the partial decay-width ratio of charm events with respect to all hadronic final-states of the Z boson, R_c. Although the sensitivity to new-physics effects in the $Zc\bar{c}$ coupling might be lower than for the beauty quark, the precision at FCC-ee might reveal tiny deviations from the SM prediction.

Principle equations In contrast to R_b, the double-tag equations are extended in case for R_c to account for the possibly largest fraction of misidentification in $Z \to b\bar{b}$ events

$$\begin{aligned}
\text{Single } c\text{-tag:} \quad & N_{\mathrm{ST}}^c = 2N_Z \cdot (R_c\varepsilon_c^c + R_b\varepsilon_b^c + R_{uds}\varepsilon_{uds}^c) \\
\text{Double } c\text{-tag:} \quad & N_{\mathrm{DT}}^c = N_Z \cdot (R_c(\varepsilon_c^c)^2 C_c^c + R_b(\varepsilon_b^c)^2 C_b^c + R_{uds}(\varepsilon_{uds}^c)^2 C_{uds}^c) \\
\text{Double } c\text{- and } b\text{-tag:} \quad & N_{\mathrm{DT}}^{cb} = N_Z \cdot (R_c\varepsilon_c^c\varepsilon_c^b C_{cb}^c + R_b\varepsilon_b^b\varepsilon_b^c C_{bc}^c)
\end{aligned} \tag{2.1}$$

In Eq. (2.1), N_Z corresponds to the total hadronic fraction of $Z \to f\bar{f}$ events and ε_i^j are the efficiencies to tag a flavour j of a quark flavour i. This set of equations allows to simultaneously measure R_c, ε_c^c and ε_b^c, while the remaining inputs have to be determined either from Monte-Carlo simulation or directly from data in the case of R_b and ε_b^b via, for example, the exclusive b-hadron reconstruction presented in Ref. [4]. Furthermore, the efficiency correlation of the hemispheres, quantified by $C_{i(j)}^c$, requires a precise control at

unity, which has been validated in Ref. [4]. Since the effect of gluon splitting is negligible compared to the impact of misidentification, ε_c^b and ε_{uds}^c are assumed to be zero.

3 New tagging method

Former measurements of R_c at LEP and SLD have used the production rates of charm hadrons such as $D^{*\pm}$ mesons from c- and b-quarks or inclusive tags which used secondary-vertex masses or high-energetic leptons from heavy-hadron decays [5–7]. However, in order to double-tag events with reconstructed charm-hadrons in both hemispheres, the event statistics available were simply too low.

Since the background contamination from ε_i^c is itself a source of systematic uncertainty, a balanced trade-off must be found between the loss in statistical precision and reduction in systematic uncertainty from high-purity charm tags. At FCC-ee with a projected number of Z-boson decays of the order 10^{12}, an ultra-pure selection of candidates from about 20 charm-hadron decay modes has the potential to reach an unprecedented precision for R_c and possibly A_{FB}^c.

For the sake of the feasibility study of this approach, the $\bar{D}^0 \to K^+\pi^-$ mode has been chosen to be exclusively reconstructed from a sample of $8 \cdot 10^7$ $Z \to q\bar{q}$ in the IDEA detector concept [8]. The detector comprises a silicon vertex detector positioned near the beam pipe, a drift chamber for almost continuous tracking of charged particles, and a finely segmented crystal calorimeter to measure electromagnetic showers. Additionally, a dual-readout (DR) calorimeter utilises scintillation and Cerenkov fibres to measure hadronic showers. In a variant of this concept, both electromagnetic and hadronic showers are measured in the DR fibre calorimeter.

The tools from the `DELPHES` [9, 10] software toolkit have been used to find a common vertex of a charged kaon and pion track. Candidates with a vertex quality $\chi^2/n_{\mathrm{dof}} > 25$ and with an invariant mass outside of $(1850 \leq m([K^+\pi^-]) \leq 1880)\,\mathrm{MeV}$ have been discarded. Furthermore, a 100 % probability of particle identification for the final-state particles has been assumed.

4 Performance of the tagger

The performance of the tagger has been evaluated using the invariant-mass spectrum as a figure of merit to quantify reconstruction efficiencies and background contamination. Therefore, each event has been weighted according to the probability of production R_q. The kinematic properties of the $\bar{D}^0$ candidates have been used to purify the selection. First, the background from uds-quark events has been reduced since $\bar{D}^0$ are only formed from gluon splitting events in which the $g \to c\bar{c}$ hadronises to a $\bar{D}^0$ meson and falls in the signal region. Therefore, the momentum is expected to be much softer for these events, which is presented in the right panel of Fig. 1. An additional cut on the scaled $\bar{D}^0$ pointing angle $\log(1-\Omega)$ with respect to $(0,0,0)^\top$ has been applied. Here, Ω is defined via

$$\Omega = \frac{\boldsymbol{v}_{\bar{D}^0} \cdot \boldsymbol{p}_{\bar{D}^0}}{|\boldsymbol{v}_{\bar{D}^0}| \cdot |\boldsymbol{p}_{\bar{D}^0}|}\,, \tag{4.1}$$

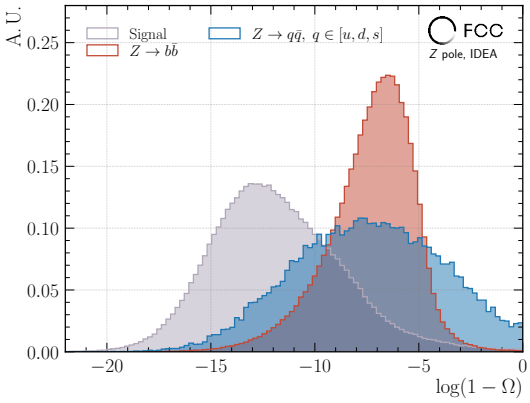

(a) The scaled pointing angle $\log(1-\Omega)$ allows for a discrimination of signal and background events, especially the one from $Z \to b\bar{b}$ events.

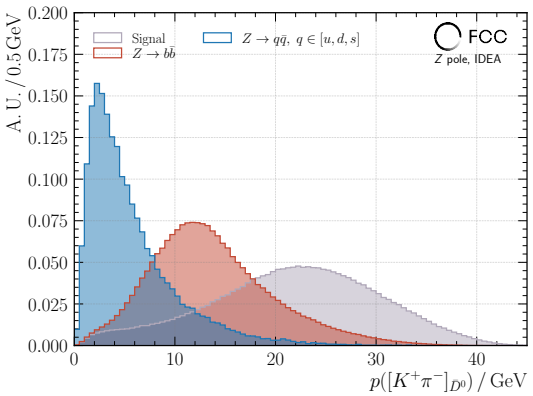

(b) The momentum distribution of the $\bar{D}^0$ candidates allows to eliminate the background contamination from light-quark physics events, which enter the signal region via gluon splitting. These candidates are expected to have less energy.

Figure 1: Distributions of the most discriminative variables in order to purify the event selection of $\bar{D}^0$ candidates.

with $\boldsymbol{v}_{\bar{D}^0}$ being the reconstructed $\bar{D}^0$ decay vertex and the $\bar{D}^0$ momentum vector $\boldsymbol{p}_{\bar{D}^0}$. This discriminator aims at reducing background contamination from $Z \to b\bar{b}$ events, where c-mesons stem from $b \to c$ transitions and are expected to not point to the interaction region. The distribution of $\log(1-\Omega)$ is shown in the left panel of Fig. 1. For the selection, $\bar{D}^0$ candidates have to pass the requirements

$$\log(1-\Omega) < -9.2 \quad \text{and} \quad p_{\bar{D}^0} > 16\,\text{GeV}\,.$$

The impact of these cuts is illustrated in Fig. 2, which shows the composition of candidates in the $\bar{D}^0$ mass region before (left plot) and after cuts (right plot). A significant reduction of the $Z \to b\bar{b}$ background can be seen and almost no light-quark physics background remains in the region of interest. The purity of $Z \to c\bar{c}$ events increases from about 29 % (before cuts) up to 86 % (after cuts).

4.1 Tagging efficiencies

The tagging efficiencies have been calculated after the application of kinematic cuts as outlined above. Their values result to

$$\varepsilon_c^c = 0.004\,57 \pm 0.000\,01\,, \quad \varepsilon_b^c = 0.000\,698 \pm 0.000\,005\,, \quad \varepsilon_{uds}^c = (3.51 \pm 0.12) \cdot 10^{-5}\,. \tag{4.2}$$

From these efficiencies it becomes clear that the light-quark flavour background is suppressed by about two orders of magnitude, allowing to assume $\varepsilon_{uds}^c = 0$ in Eq. (2.1), while the $Z \to b\bar{b}$ background has a sizeable contribution.

With the stated efficiencies and a foreseen number of hadronic Z-boson decays of $N_Z = 4.2 \cdot 10^{12}$, the statistical precision of R_c has been calculated to

$$\sigma_{\text{stat.}}(R_c) = 5.3 \cdot 10^{-5}\,, \tag{4.3}$$

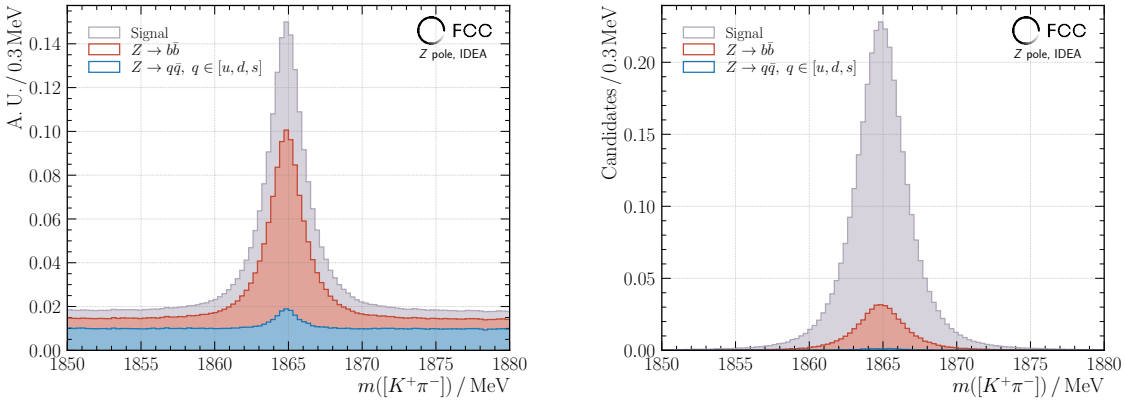

(a) Before any cuts.

(b) After kinematic cuts.

Figure 2: The stacked invariant-mass distribution in the region-of-interest before and after kinematic cuts in Fig. a and Fig. b, respectively.

which translates in an improvement of about a factor 60 compared to the statistically most precise measurement from the SLD Collaboration [11].

5 Systematic uncertainties

One of the main advantages of the exclusive b-hadron reconstruction for R_b is the cancellation of background efficiencies. Their origin contributed to the leading fraction in the systematic uncertainty budget. Although ε_{uds}^{c} can be safely set to zero, the impact of ε_{b}^{c} becomes non-negligible if $\sigma_{\text{stat.}}(R_c) \approx \sigma_{\text{syst.}}(R_c)$ is targeted. However, the nominal value of ε_{b}^{c}, as well as its precision, are sources of a systematic uncertainty component, and the goal must be the minimisation of ε_{b}^{c} to reduce its impact on $\sigma_{\text{syst.}}(R_c)$. Furthermore, the hemisphere efficiency correlation $C_{i(j)}$ is another source of systematic uncertainty, which is briefly discussed in Sec. 5.2.

5.1 Uncertainty from misidentification

From the set of Eqs. (2.1) the impact of ε_{b}^{c} on the uncertainty of R_c can be calculated. For this, the precision of ε_{b}^{c} is computed from N_{DT}^{cb} in Eq. (2.1), assuming $\varepsilon_{c}^{b} = \varepsilon_{c}^{uds} = 0$. The remaining inputs R_b and ε_{b}^{b} are taken from the current estimate of the total uncertainty in reach for R_b using the exclusive b-tagger

$$R_b = 0.216\,00 \pm 0.000\,03\,, \quad \varepsilon_{b}^{b} = 0.010\,000 \pm 0.000\,002\,. \tag{5.1}$$

From this, the uncertainty on ε_{b}^{c} follows to

$$\varepsilon_{b}^{c} = (6977 \pm 3) \cdot 10^{-7}\,.$$

Finally, it allows to compute the systematic uncertainty arising from the contamination of $Z \to b\bar{b}$ events to be

$$\sigma_{\text{syst.}}(\text{from } \varepsilon_{b}^{c}) = 2.7 \cdot 10^{-6}\,,$$

which is about a factor of 20 below the statistical precision. Furthermore, this enables direct assessment of the systematic uncertainty for R_c originating from the total uncertainty of R_b. The dependence is presented in Fig. 3a, where the current estimate of R_b from Eq. (5.1) is highlighted in darkred. With the level of precision in reach for R_b, the difference to the statistical uncertainty of R_c is at least one order of magnitude and is no limiting factor in the measurement of R_c. Systematic uncertainties from R_{uds} are not considered here due to the smallness of ε^c_{uds}. While this study focusses on a rather simple decay mode,

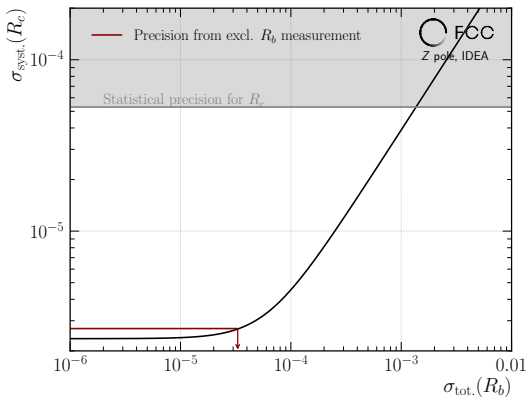

(a) Systematic uncertainty on R_c arising from the total uncertainty of R_b, which drives the precision in the determination of ε^c_b.

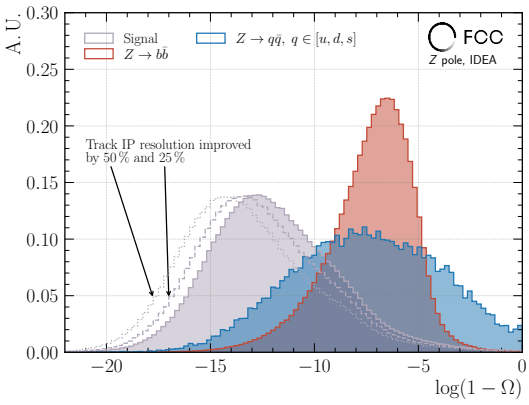

(b) An improved impact-parameter resolution by 25 % (dashed) and 50 % (dotted) increases the separation power from background events. This might become relevant for specific, more complex charm decay modes.

Figure 3: The systematic uncertainty on R_c as a function of the precision on R_b in the left panel and the impact of an improved impact-parameter resolution on the signal-background separation in the right one.

more complex ones including also neutral hadrons in the final state might need a more sophisticated signal-background separation. Here, potential detector requirements from an improved (longitudinal and transverse) impact parameter resolution can be derived which would suppress potentially toxic backgrounds from $Z \to b\bar{b}$ events in the $\log(1-\Omega)$-variable distribution. The result is shown in Fig. 3b, where two scenarios of improvement have been assumed.

5.2 Uncertainty from hemisphere correlation

As already pointed out in Ref. [4], the size of the hemisphere efficiency correlation is itself a source of systematic uncertainty, which needs to be controlled at unity. For consistency with Ref. [4], the notation $\Delta C^c_i = 1 - C^c_i$ is used in the following. In Fig. 4 the total uncertainty on R_c, computed as $\sigma_{\text{tot.}}(R_c) = \sqrt{\sigma_{\text{stat.}}(R_c)^2 + \sigma_{\text{syst.}}(R_c, \text{ from } C^c_i)}$, is shown as a function of the relative precision on ΔC^c_i. In the plot, also the current precision of R_c is presented as grey area. It can be seen that the nominal value of ΔC^c_i has a significant effect on the uncertainty of R_c. However, in Ref. [4] it has been shown, that the dominant source of

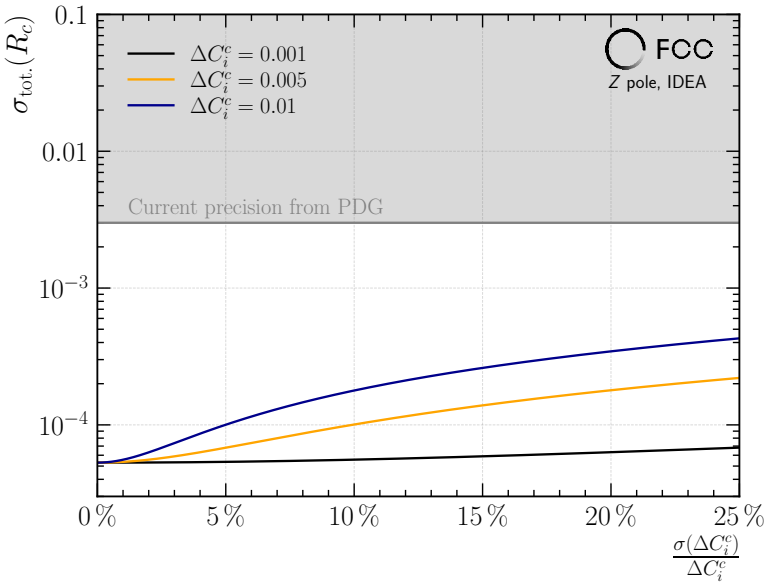

Figure 4: Impact of the nominal value of the hemisphere efficiency correlation on the total uncertainty of R_c (different colours). Furthermore, a scan over the relative uncertainty of the hemisphere correlation is shown.

$\Delta C_i^c \neq 0$ originating from the reconstruction of a common primary event vertex can be eliminated by a simple selective cut in the beam-interaction region. For further details, the reader is advised to check Ref. [4]. There, an inclusive value of the hemisphere efficiency correlation of 0.001 ± 0.003 has been found (black line in Fig. 4). The uncertainty only corresponds to the limited number of simulated events available. It can be concluded that with a similar approach, the systematic uncertainty arising from ΔC_i^c is no limiting factor if determined with a relative precision of at least 5 % from Monte-Carlo simulations.

Finally, it can be concluded that the background contamination from $Z \to b\bar{b}$ events does not limit the precision of R_c. However, the hemisphere efficiency correlation might be yet again a limiting factor for the precision of R_c if not controlled around zero.

It is mentioned here that the studies are only based on the $\bar{D}^0 \to K^+\pi^-$ decay mode. More fully-charged decay modes would further improve the statistical precision, but would also require to reevaluate systematic uncertainties. From the studies outlined here, the preliminary uncertainties for R_c result to

$$R_c = \mu(R_c) \pm 5.3 \cdot 10^{-5}(\text{stat.}) \pm 5.4 \cdot 10^{-5}(\text{syst.})\,, \tag{5.2}$$

combining the systematic uncertainty from b misidentification and from ΔC_i^c for a relative precision of 5 %.

6 A_{FB}^{c} from exclusive c-hadron decays – the idea

Based on the idea of measuring R_c with exclusively reconstructed c-hadrons, the concept is applied to the measurement of the c-quark forward-backward asymmetry, A_{FB}^c. Conceptually,

it follows the analysis outlined in Ref. [4]. For the sake of this study, the fully charged c-meson decay $D^+ \to K^-2\pi^+$ is used as hemisphere flavour and charge tagger. It also serves as a direction estimator of the c quark. Although mixing of neutral charm mesons is a minor effect that would be avoided by considering only the charged D-meson decay, it furthermore avoids double-Cabibbo suppressed decays in e. g. $\bar{D}^0 \to K^+\pi^-$ decays.

$D^+ \to K^-2\pi^+$ candidates have been reconstructed from $Z \to q\bar{q}$ events produced with `PYTHIA8` and propagated through the IDEA detector concept with `DELPHES` to evaluate the performance. In this short section, only the statistical precision is presented since the evaluation of the systematic uncertainty is still work in progress. However, it has been assumed, based on the studies in Ref. [4], that the leading systematic uncertainty, originating from high-energetic gluon radiation in the initial state (QCD corrections), can be mitigated by an energy cut on the D^+ candidates. The energy cut has several effects: first, it significantly reduces the contamination from background events stemming either from $b \to c$ transitions or from gluon-splitting events with $g \to c\bar{c}$. Second, the impact of QCD corrections on the systematic uncertainty reduces up to a level until it does not longer limit the precision of A^c_{FB}. Third, the direction estimation of the c-quark from the D^+ direction of flight, a crucial observable to identify forward and backward events, becomes more accurate in the presence of c-hadron energy cuts.

Motivated by the results in Ref. [4], an energy cut of $E(D^+) > 35\,\mathrm{GeV}$ has been applied to the reconstructed candidates, which results in a statistical uncertainty for A^c_{FB} of

$$\sigma_{\mathrm{stat.}}(A^c_{\mathrm{FB}}) = 1.8 \cdot 10^{-5}\,. \tag{6.1}$$

A precise determination of the systematic uncertainties is work in progress. However, no significant showstoppers are expected to achieve a commensurate systematic precision.

7 Measurement of R_s and A^s_{FB} – the idea

While strange-quark tagging becomes more challenging with state-of-the-art multivariate approaches, the exclusive reconstruction of strange hadrons can be a valuable hemisphere flavour and charge tagger. In this section, the idea of measuring R_s and A^s_{FB} with exclusively reconstructed strange hadrons is presented. For R_s, the concept using candidates $\phi(1020)$ is shown below, and a measurement concept for A^s_{FB} with Ξ^- is presented in Sec. 7.2.

7.1 R_s measurement

The set of equations adapts accordingly to

$$\begin{aligned} \text{Single } s\text{-tag:} \quad & N^s_{\mathrm{ST}} = 2N_Z \cdot (R_s\varepsilon^s_s + R_c\varepsilon^s_c + R_b\varepsilon^s_b + R_{ud}\varepsilon^s_{ud}) \\ \text{Double } s\text{-tag:} \quad & N^s_{\mathrm{DT}} = N_Z \cdot (R_s(\varepsilon^s_s)^2 C^s_s + R_c(\varepsilon^s_c)^2 C^s_c + R_b(\varepsilon^s_b)^2 C^s_b + R_{ud}(\varepsilon^s_{ud})^2 C^s_{ud}) \end{aligned} \tag{7.1}$$

For R_s, the $\phi(1020)$ meson has been chosen as a possible strange hadron to tag $Z \to s\bar{s}$ events, since no charge information is required. In about 50 % of the cases, it decays to a pair of charged kaons. To verify the feasibility of the approach, about $2 \cdot 10^9$ $Z \to q\bar{q}$ events have been used from the `winter2023` campaign, which have been generated and

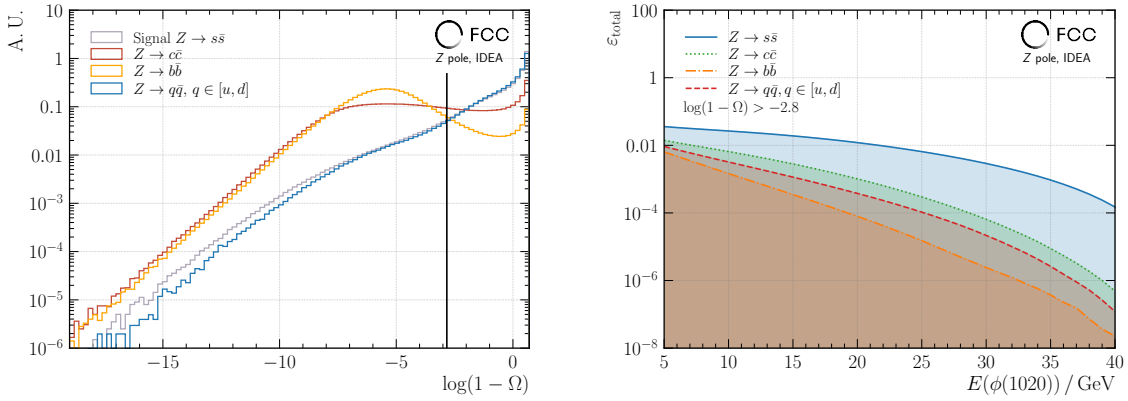

(a) A cut in $\log(1 - \Omega)$ can be used to further suppress the leading background from $Z \to c\bar{c}$ events.

(b) The total efficiencies splitted by flavour as a function of the $\phi(1020)$-meson energy.

Figure 5: A cut on the scaled pointing angle $\log(1 - \Omega)$ significantly reduces the contamination from heavy-quark backgrounds (see left panel). The total efficiency as a function of the energy is shown in the right panel.

hadronised with `PYTHIA`. The detector response has been modelled with `DELPHES` and the IDEA detector card. Tracks for the reconstruction of the $\phi(1020)$ meson have been selected outside of the beam-interaction region. The principle of this method is described in further detail in Ref. [4]. $\phi(1020)$ candidates have been reconstructed using 100 % particle-ID information and by vertexing a pair of oppositely charged kaons to a common vertex. The invariant mass of the reconstructed vertex must lie in between 1 GeV and 1.04 GeV and its vertex χ^2/n_{dof} must be smaller than 10. Since the hadronisation fractions are unknown to date for $s \to \phi(1020)$, the statistical precision in R_s is fully based on the one provided internally by `PYTHIA`.

In order to reduce background contamination from non-signal candidates, again a $\log(1 - \Omega)$ cut has been applied. Its distribution is presented in the left panel of Fig. 5a and the candidates have to fulfil $\log(1 - \Omega) > -2.8$. For this cut and an energy of the $\phi(1020)$ candidates above 20 GeV, the total efficiencies have been found to be

$$\varepsilon_s^s = 0.012\,018 \pm 0.000\,005\,, \qquad \varepsilon_c^s = 0.001\,017 \pm 0.000\,001\,, \tag{7.2}$$

$$\varepsilon_b^s = (6.98 \pm 0.04) \cdot 10^{-5}\,, \qquad \varepsilon_{ud}^s = 0.000\,378 \pm 0.000\,001\,. \tag{7.3}$$

A suitable cut on the energy can be extracted by a simultaneous examination of the systematic uncertainty arising from the background contamination. For this, a similar approach is followed as for the measurement of R_c. From the estimated uncertainties of R_b and R_c, the respective precision of the background efficiencies ε_b^s and ε_c^s can be calculated. Then, the systematic uncertainty for each background flavour can be computed. For the light-quark backgrounds, R_{ud} and ε_{ud}^s have been assumed to be

$$R_{ud} = (1 - R_b - R_c - R_s) \pm 0.01\,, \quad \varepsilon_{ud}^s = 3 \cdot 10^{-4}\,. \tag{7.4}$$

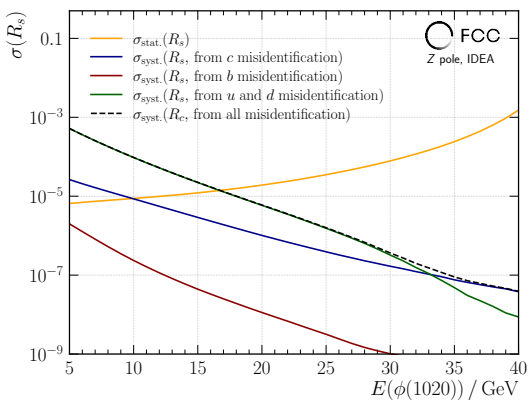

(a) The statistical and systematic uncertainties of R_s as a function of the $\phi(1020)$-meson energy. An opportunistic cut at $E(\phi(1020)) > 20\,\text{GeV}$ has been chosen.

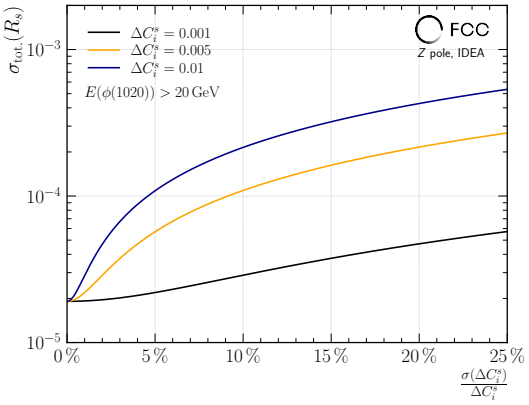

(b) The total uncertainty as a function of the relative precision of the hemisphere efficiency correlations.

Figure 6: Statistical and systematic uncertainty evaluation: as a function of the $\phi(1020)$-meson energy in the left panel and as a function of the hemisphere efficiency correlation in the right panel.

The choice of ε_{ud}^s is motivated by a simple and very preliminary study of a possible measurement of R_{ud} with beam-like $\pi^+ = |u\bar{d}\rangle$ as a light-quark tagger. The uncertainty estimate of R_{ud} is a conservative one to verify the feasibility of the measurement of R_s with $\phi(1020)$ mesons. The different uncertainty components as a function of the $\phi(1020)$-meson energy is shown in Fig. 6a. It can be seen that R_{ud} is the leading source of systematic uncertainty over nearly the entire energy spectrum, while ε_c^s and especially ε_b^s have minor impact. Furthermore, it has been verified that the precision on R_{ud} drives the uncertainty on R_s. However, for energies roughly above 20 GeV the systematic uncertainties become subdominant compared to the statistical one. With this energy cut, the statistical precision on R_s follows to

$$\sigma_{\text{stat.}}(R_s) = 2 \cdot 10^{-5}\,. \tag{7.5}$$

Furthermore, and similar to the approach followed for R_c, the impact of the hemisphere efficiency correlation has been evaluated. Again, the total uncertainty stated on the y-axis of Fig. 6b results from $\sigma_{\text{tot.}} = \sqrt{\sigma_{\text{stat.}}(R_s)^2 + \sigma_{\text{syst.}}(R_s, \text{ from } C_i^s)}$. It becomes clear that the hemisphere efficiency correlation is the leading source of systematic uncertainty for the measurement of R_s. However, with the nominal value of the hemisphere efficiency correlation in reach extracted from the measurement of R_b and a relative precision of 5 %, it gives

$$R_s = \mu(R_s) \pm 2 \cdot 10^{-5}(\text{stat.}) \pm 2 \cdot 10^{-5}(\text{syst.})\,. \tag{7.6}$$

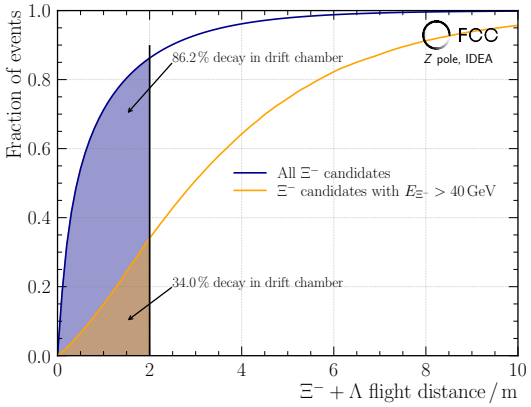

(a) Only a fraction of candidates of about 34 % with energies of at least 40 GeV decays within the volume of the drift chamber.

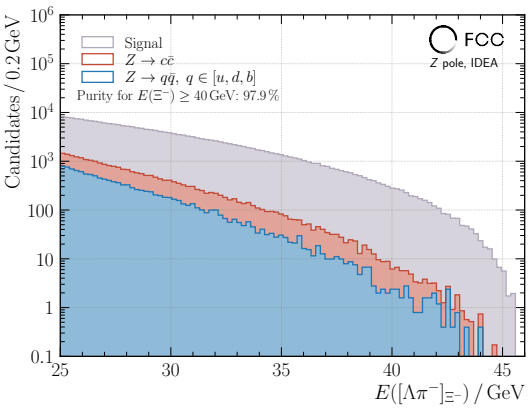

(b) From the energy distribution, the purity can be estimated to be around 98 % for beam-like Ξ^- candidates.

Figure 7: A significant efficiency loss is due to the finite size of the drift chamber, which is needed to resolve all final-state particles, also from the decay of the Λ baryon. Nevertheless, these high-energetic candidates are needed to reach purities of about 98 %.

7.2 A^s_{FB} measurement

For A^s_{FB}, charge and direction information is required in addition to a flavour tag. Therefore, the Ξ^- baryon serves as a possible strange tagger. However, the reconstruction of a beam-like Ξ^- baryon in its predominant decay channel $\Xi^- \to [p\pi^-]_\Lambda \pi^-$ is not straightforward due to the very long lifetime of the Ξ^- baryon of the order 10^{-10} s. In turn, this means that it flies on average about 1.5 m and may escape detection in the drift chamber, given that the Λ baryon lives on the same timescale.

The remaining fraction of candidates that actually fulfil the requirement of completely decaying within the radius of the drift chamber is presented in the left panel of Fig. 7. Due to the correlation of flight distance and particle energy, the fraction of remaining events is reduced to about 34 % after setting a lower energy cut of $E(\Xi^-) = 40$ GeV. With this energy cut, the purity results in 98 %. However, all final-state particles must be measured to increase the probability of identifying the Ξ^- track through a common vertex in the drift chamber. Studies must examine the possibility of a late V^0 reconstruction and the kink produced by the Ξ^- decay. For the sake of this study, only the produced Monte-Carlo Ξ^- candidates have been used in addition to an assumed reconstruction efficiency of 50 %. With these assumptions, a statistical precision of A^s_{FB} of

$$\sigma_{\mathrm{stat.}}(A^s_{\mathrm{FB}}) = 2 \cdot 10^{-4}\,, \tag{7.7}$$

might be in reach. Again, the reader is reminded that the hadronisation fractions are unknown to date and drive the statistical precision. For the studies presented here, the default hadronisation fractions of `PYTHIA` have been taken. A study of the systematic uncertainties is subject of future work.

8 Conclusions

This note has presented the use of exclusively reconstructed charm-hadrons to measure R_c and possibly $A_{\mathrm{FB}}^{\mathrm{c}}$. The performance of the tagger has been evaluated on reconstructed $\bar{D}^0$ candidates in the $K^+\pi^-$ decay channel and the main contamination arises from $Z \to b\bar{b}$ events. However, the main source of systematic uncertainty, similar to R_b, remains the correlation of hemisphere efficiencies. Its precise knowledge ensures a commensurate systematic uncertainty with respect to the statistical one. For both observables, a precision of the order 10^{-5} is within reach.

Finally, the measurement principle has been extended to strange quarks, enabling the measurement of R_s and $A_{\mathrm{FB}}^{\mathrm{s}}$ with precisions of the order 10^{-5} and 10^{-4}, respectively. Although the experimental feasibility must be proven in the next step.

References

[1] ATLAS Collaboration, *Observation of a new particle in the search for the Standard Model Higgs boson with the ATLAS detector at the LHC*, Physics Letters B **716** (2012) 1, ISSN: 0370-2693, DOI: https://doi.org/10.1016/j.physletb.2012.08.020.

[2] CMS Collaboration, *Observation of a new boson at a mass of 125 GeV with the CMS experiment at the LHC*, Physics Letters B **716** (2012) 30, ISSN: 0370-2693, DOI: https://doi.org/10.1016/j.physletb.2012.08.021.

[3] A. Abada et al., *FCC-ee: The Lepton Collider*, The European Physical Journal Special Topics **228** (2019) 261, DOI: 10.1140/epjst/e2019-900045-4.

[4] L. Röhrig et al., *Measuring A_{FB}^b and R_b with exclusive b-hadron decays at FCC-ee*, 2025, arXiv: 2502.17281 [hep-ex].

[5] OPAL Collaboration, *Measurement of $f(c \to D^*+X)$, $f(b \to D^*+X)$ and $\Gamma(c\bar{c})/\Gamma(q\bar{q})$ using $D^{*\pm}$ mesons*, Eur. Phys. J. C **1** (1998) 439, DOI: 10.1007/s100520050095, arXiv: hep-ex/9708021.

[6] DELPHI Collaboration, *Measurements of the Z partial decay width into c anti-c and multiplicity of charm quarks per b decay*, Eur. Phys. J. C **12** (2000) 225, DOI: 10.1007/s100529900228.

[7] ALEPH Collaboration, *Study of charm production in Z decays*, Eur. Phys. J. C **16** (2000) 597, DOI: 10.1007/s100520000421, arXiv: hep-ex/9909032.

[8] The IDEA Study Group, *The IDEA detector concept for FCC-ee*, 2025, arXiv: 2502.21223 [physics.ins-det].

[9] The DELPHES 3 Collaboration, *DELPHES 3: a modular framework for fast simulation of a generic collider experiment*, Journal of High Energy Physics **2014** (2014) 57, DOI: 10.1007/JHEP02(2014)057.

[10] F. Bedeschi, *A vertex fitting package* (2024), DOI: 10.17181/HVCPV-BK752.

[11] SLD Collaboration, *Measurement of the branching ratio of the Z^0 into heavy quarks*, Phys. Rev. D **71** (2005) 112004, DOI: 10.1103/PhysRevD.71.112004, arXiv: hep-ex/0503005.